Quantization of pH: Evidence for Acidic Activity of Triglyceride Lipases†

Kristian R. Poulsen,‡ Torben Snabe,‡ Evamaria I. Petersen,‡ Peter Fojan,‡ Maria T. Neves-Petersen,‡ Reinhard Wimmer,§ and Steffen B. Petersen*,‡

Biostructure and Protein Engineering Group, Department of Physics and Nanotechnology, Aalborg University, Dk-9220 Aalborg, Denmark, and Department of Life Sciences, Aalborg University, Dk-9000 Aalborg, Denmark

Received April 6, 2005; Revised Manuscript Received June 17, 2005

ABSTRACT: Here we present a study of lipolytic activity of lipases from *Fusarium solani* pisi (cutinase), *Rhizomucor miehei*, *Pseudomonas cepacia*, and *Humicola lanuginosa*. Their activities toward triolein provide clear evidence for considerable enzymatic activity under acidic conditions. The activity was followed using Fourier transform infrared attenuated total reflection (FTIR-ATR) and nuclear magnetic resonance (NMR). Using these approaches, all the lipases that were studied exhibited lipolytic activity down to pH 4. The common model for the catalytic activity of the *F. solani* pisi cutinase, and lipases in general, requires the deprotonation of the active site histidine. Measurements using ^{13}C NMR spectroscopy showed a pK_a value in the absence of substrate that is not consistent with the detected acid activity. We propose a novel model for the electrostatics in the active site of cutinase that could explain the observed acidic activity. The active site is essentially covered with the lipid surface during catalysis, thus preventing chemical communication between the active site and the bulk solvent. We propose that the classical definition of pH in bulk solution is not applicable to the active site environment of a lipase when the active site is inaccessible to solvent. In small restricted volumes, the pH must be quantized, and since much of the biological world is dependent on compartmentalization of processes in small volumes, it becomes relevant to investigate when this mechanism comes into play. We have made a quantitative assessment of how large the restricted volume can be and still lead to quantization of pH.

Lipases and esterases have received more attention over the past decades. These enzymes are relatively stable and capable of catalyzing a variety of reactions, including the degradation of triacylglycerols. They are important for diverse industrial applications, such as detergent enzymes, and the value of lipases produced in 2000 worldwide was estimated to be $1.5 billion (*1*). The known lipases are water-soluble enzymes that display hydrolytic activity toward a wide range of poorly water-soluble esters. They share a common α/β-hydrolase fold and a catalytic triad (Ser-His-Asp/Glu) in the active site of the enzyme (*2*). Some of them have a lid, which consists of a flexible helix or flexible loop that covers the active site. The current paradigm includes the lid being closed until the enzyme binds to the lipidic surface (*3*). At this point, the low dielectric constant of the lipidic environment triggers an opening of the lid, which exposes a number of hydrophobic residues that assist in the docking of the enzyme to the interface (*4*, *5*).

Many lipases share this so-called interfacial activation. Three of the lipases used in this study belong to that group. These are lipases from *Pseudomonas cepacia* (*6*), *Rhizomucor miehei* (*7*), and *Humicola lanuginosa* (*8*). The fourth lipase used in this study, cutinase from *Fusarium solani* pisi (*9*, *10*), does not display any lid, but clearly adheres to lipidic surfaces. Because of its lack of interfacial activation, it is also often termed an esterase (*11*). The lipases were previously cloned and characterized in terms of their substrate profile as well as some structural aspects: *P. cepacia*, PDB entry 3LIP (*12*); *R. miehei*, PDB entry 3TLG (*13*); and *H. lanuginosa*, PDB entry 1DTE (*14*). Even though they all display a hydrolytic activity toward a broad variety of esters ranging from partially soluble *p*-nitrophenyl esters to insoluble long-chain triglycerides, they exhibit a preference for short-chain fatty acid esters (*6*, *15*−*17*). All four lipases display their pH optima in the alkaline pH range (*17*, *18*); cutinase, for instance, exhibits its highest activity toward tributyrin at pH ∼8.5 (*19*).

The most commonly used method for determining the enzymatic activity of triacylglycerol lipases is the pH-stat method, which was first described in 1961 by Desnuelle (*20*). This method can be used in the neutral and alkaline pH range, where the free fatty acid released by lipolytic activity is deprotonated. Titration of the released protons is taken as a measurement for enzymatic activity. There are some distinct limitations to this method. First, the reaction takes place in a lipid/water emulsion environment, which may not resemble the conditions under which hydrolysis is performed in application situations. Second, it cannot be used in real time measurements at a pH lower than the pK_a value of the product, since the method relies on the detection of the protons released from the fatty acid. Using short-chain triglycerides, such as triacetin or tripropion, this allows for measurements in the range above the pK_a of the acetic acid

† This work has been supported by a grant from the Lundbeck Foundation (Denmark), The Danish Research Council (Innovation Post Doc program), Novozymes, and Novo Nordic.

* To whom correspondence should be addressed. Telephone: (+45) 9635 8469. Fax: (+45) 9815 6502. E-mail: sp@nanobio.auc.dk.

‡ Department of Physics and Nanotechnology.

§ Department of Life Sciences.

10.1021/bi050634o CCC: $30.25
Published on Web 08/05/2005

(4.7) and propionic acid (4.9). The range for measurement with long-chain triglycerides is much narrower with the following pK_a values reported for some long-chain fatty acids: 8.6−8.8 for palmatic acid (*21*), 9.0 for stearic acid (*22*), and 9.85 for oleic acid (*23*) under lipid/water emulsion conditions. These values must be expected to be dependent on the presence of salt in the aqueous solution. We have estimated the pK_a of oleic acid to be around 8 under experimental lipid/water emulsion conditions (results not shown) and to be between 7 and 8 under the conditions used for the FTIR experiments (*24*). Acid activity can be measured by the pH-stat method but not in real time; bringing a sample of the reaction mixture to a pH value above the pK_a of the fatty acid makes it possible to calculate the amount of fatty acid released until this point, and in effect determine the activity at a pH lower than the pK_a of the substrate.

Another favored lipase activity assay is that of using *p*-nitrophenyl esters to monitor catalytic activity (*25*), the reason being the convenient spectroscopic detection of the *p*-nitrophenyl products of the degradation. This makes this assay useful for fast detection and evaluation of enzyme activity. But the *p*-nitrophenyl esters do not resemble the natural substrate in any way apart from the esterified fatty acid. A drawback to this method is that many classical lipases do not show any significant activity toward soluble *p*-nitrophenyl esters. Also, the coloring of the *p*-nitrophenol in solution is heavily dependent on the pH, and at acidic pH, the coloring is no longer present (*26*). This makes this method a poor choice for direct detection of lipase activity at acidic pH.

Here we apply an attenuated total reflection Fourier transformed infrared (ATR-FTIR)[1] method (*27*), in cooperation with proton NMR, to document enzymatic activity at acidic pH. ATR-FTIR can be used to assess the real time interfacial enzymatic activity of lipases over a pH range that is wider than that which can be accessed by the pH-stat method. A key reason for this observation is that the ATR-FTIR and NMR methods both allow a direct spectroscopic observation of both substrate and products regardless of the pH of the solution. Triacylglycerol hydrolysis degrades ester linkages, releasing fatty acids from the glycerol skeleton; thus, for the ATR-FTIR, the specific carbonyl ester absorption frequency ($\approx$1745 cm^{-1}) can be used for this purpose. For the detection with NMR spectroscopy, the signals stemming from the glycerol backbone hydrogen atoms are ideal for following the hydrolysis. Detection of enzymatic activity using the ATR-FTIR and NMR methods is not dependent on the protonation state of the products, like the pH-stat method is, and allows detection of the hydrolysis of the natural substrate.

A reason lipase activity under acidic conditions is generally considered unlikely is that the current model for the lipolytic mechanism assumes that the active site histidine is in its deprotonated state. The average pK_a of histidine in proteins has been reported by Edgcomb and Murphy to be 6.6 $\pm$ 1 (*28*), but with pK_a values reported to be lower than 2.3 in some extreme cases (*29*). Previously, the pK_a of the active site histidine (His188) side chain of cutinase has been reported to be 5.9 (*30*). To explain the acid activity of lipases, the pK_a of the active site histidine must be considerably lower than that reported or we must revise the model used for understanding lipase activity. The reported determination of the pK_a of His188 was carried out by monitoring H^N and backbone ^{15}N chemical shifts in the NMR spectra for the NH pairs close to His188 (*30*). Since the backbone $N-H^N$ pairs are situated relatively far from the protonation/deprotonation site in the histidine and the observed effects consequently are very weak, we chose to utilize the chemical shift of the His188 $C^{\epsilon 1}-H^{\epsilon 1}$ pair, which, because of its position as next neighbor to the protonation/deprotonation site, is the optimal probe for detection of the pK_a value of any histidine.

EXPERIMENTAL PROCEDURES

ATR-FTIR Measurements. Hydrolytic activity measurements of four different lipases [cutinase from *F. solani* pisi and lipases from *R. miehei* (Sigma), *P. cepacia* (Sigma), and *H. lanuginosa* (Lipolase TM, kindly supplied by S. Patkar and K. Borch, Novozymes)] were performed on an ATR-FTIR spectrometer (Bruker model IFS 66V/S) with a DTGS detector (a pyroelectric device incorporating deuterium triglycine sulfate in a temperature-resistant alkali halide window) from Bruker, using triolein as a model substrate. The substrate (99% triolein, Fluka) was applied onto a 45° ZnSe ATR crystal with a surface area of 7 cm $\times$ 1 cm. The ATR crystal made out the base in a reaction chamber $\sim$0.1 cm in height and a total volume of $\sim$1 mL. The temperature could be controlled by application of water flow from an external water bath through the ATR crystal holder.

After the film was stabilized, the lipid layer was flushed with a citrate/tris-glycine buffer (each at 50 mM, pH 3.5−10.5) several times. After an equilibration period of 4−5 min, the buffer was exchanged with the same buffer (citrate/tris-glycine buffer, each at 50 mM, pH 3.5−10.5) containing enzyme. If not stated otherwise, the enzyme concentration was 0.06 μg/mL. All experiments were performed at 25 $\pm$ 0.5 °C. Spectra were recorded before and during hydrolysis with 32 scans at 4000−800 cm^{-1} recorded with a 10 kHz scan rate and a resolution of 4 cm^{-1}. The light pathway was purged with dry nitrogen gas for removal of water vapor and CO_2. Hydrolysis of triolein was assessed as a decrease in carbonyl ester absorption (1745 cm^{-1}) in the spectrum over time. The procedure and spectrum analysis were performed according to the method of Snabe and Petersen (*27*).

Measurements of Cutinase Activity Using NMR. Analysis of the hydrolytic activity of cutinase was carried out using a Bruker DRX 600 MHz NMR spectrometer with a xyz-grad TXI (H/C/N) probe at 288 K. For measuring activity on triolein, samples were prepared by mixing a citrate/tris-glycine buffer (each at 50 mM, pH 4 and 6) with triolein and cutinase to final concentrations of 40 mM and 0.45 μM, respectively. The degradation was carried out at 25 °C, while inverting the sample to mimic the ATR-FTIR experimental procedure. At 0.5, 1, 1.5, 2, 2.5, and 3 h, aliquots were taken and prepared for NMR analysis; 500 μL of sample was shaken with 700 μL of $CDCl_3$ to extract the lipid phase. The samples were spun, and the chloroform phase was collected; to reduce water signals in the final NMR spectrum, this was then washed with 500 μL of D_2O (99% Cambridge Isotope

[1] Abbreviations: FTIR-ATR, Fourier transform infrared attenuated total reflection; NMR, nuclear magnetic resonance.

Labs) and then dried by addition of a small amount of anhydrous sodium sulfate (Sigma-Aldrich). The spectrum recorded is a one-dimensional proton spectrum using 64K data points with a spectral width of 20 ppm, recording eight scans and two dummy scans with a relaxation delay of 30 s. The long relaxation delay was chosen to rule out integration errors brought about by different relaxation times of the ^{1}H signals of different species. To detect any autohydrolysis of the sample during the reaction, samples without enzyme were left for 24 h at 25 °C before sample preparation.

To determine the pH−activity profile of cutinase on a soluble ester, samples were prepared by mixing a deuterated phosphate buffer (200 mM final concentration) with the desired pD value (3.5−9) with propyl acetate (5 mM final concentration) and adding cutinase (0.74 μM final concentration) only immediately before the start of the experiment to a final volume of 600 μL. The recorded spectrum is a pseudo-two-dimensional type experiment recording a one-dimensional (1D) NMR spectrum every 6 min. The recorded 1D proton spectrum contains 32K data points, has a spectral width of 11 ppm, and is recorded with 16 scans with a relaxation delay of 15 s.

NMR Measurements of the Cutinase His188 pK_a. Determination of the pK_a of the active site histidine from cutinase was carried out using a Bruker DRX 600 MHz NMR spectrometer with a xyz-grad TXI (H/C/N) probe at 298 K. The samples containing uniformly ^{13}C- and ^{15}N-labeled cutinase were prepared in 300 μL of phosphate buffer (20 mM) containing 5% D_2O. Prior to the individual measurements, the pH of the sample was adjusted by adding HCl or NaOH. The chemical shift of the His188 $C^{\epsilon 1}-H^{\epsilon 1}$ pair was determined from a ^{15}N-decoupled ^{1}H−^{13}C HSQC spectrum (*31*), and the INEPT delay times were optimized for the detection of the His188 $C^{\epsilon 1}-H^{\epsilon 1}$ pair. The spectrum is recorded using 4K complex data points, with a spectral width of 20 ppm, and 1K data points, with a spectral width of 13 ppm, in the direct and indirect dimensions, respectively. A total of 32 scans and dummy scans were collected per spectrum. The spectra were analyzed using XWinNMR2.6. The $C^{\epsilon 1}-H^{\epsilon 1}$ pair was identified by use of the NMR assignment published by Prompers et al. (*32*) and verified by the fact that the $C^{\epsilon 1}-H^{\epsilon 1}$ pair contains the only aromatic carbon atom lacking a neighboring carbon atom and therefore is the only carbon atom not to show *J* coupling in the indirect dimension of the HSQC spectrum. Spectra were recorded over a pH range from 3.3 to 8.4.

Production of Cutinase. Expression of the cutinase gene in *Escherichia coli* BL21(DE3), using pFCEX1 (*19*), was performed in 1 L of Luria Broth (LB) containing ampicillin (100 μg/mL). The cells were grown at 25 °C. Induction of the culture was carried out at an OD_{600} of 1.5 for ∼6 h with 0.1 mM isopropyl β-D-thiogalactopyranoside (IPTG). For the NMR measurements of the pK_a of His188, expression was performed in 0.5 L of minimal medium (M9) containing uniformly labeled [^{13}C]glucose and [^{15}N]ammonium sulfate (99%, Spectra stable isotopes), containing ampicillin (100 μg/mL). The cells were grown at 25 °C. Induction of the culture was carried out at an OD_{600} of 0.5 for ∼16 h with 0.1 mM IPTG.

Cutinase was isolated from the periplasmic space by applying an osmotic shock to the cells using a buffer containing 20% sucrose. After the cells had been washed with pure water, supernatants of the sucrose and water treatments were dialyzed against a 20 mM NaAc (pH 5) buffer. Both enzyme solutions were applied to a high-resolution strong cation-exchange column (Source 15S, Pharmacia LKB) equilibrated with 20 mM NaAc (pH 5) and eluted with the same buffer containing an increasing gradient of 0 to 1 M NaCl. Elution with ∼0.1 M NaCl allowed recovery of the purified enzyme. The purified cutinase was dialyzed against water and freeze-dried.

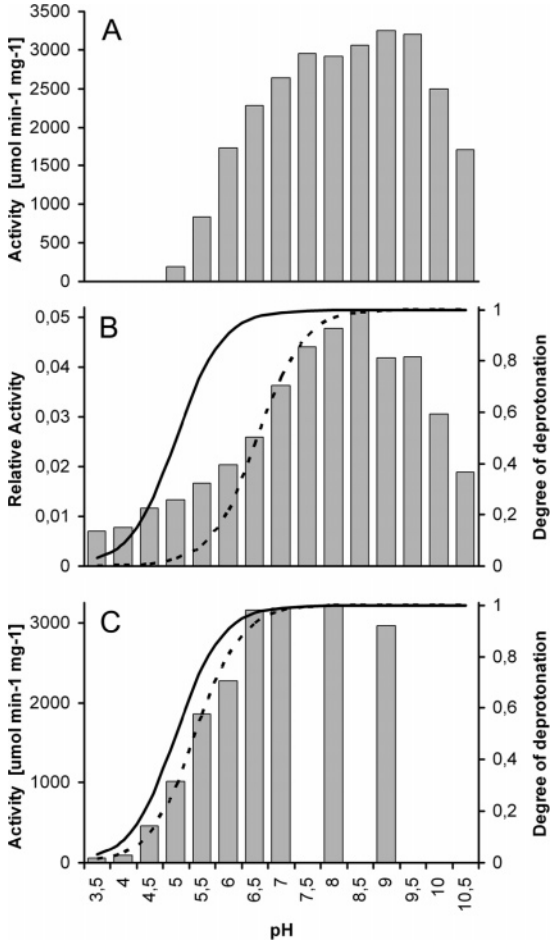

FIGURE 1: pH−activity profiles of *F. solani* pisi cutinase measured with the (A) pH-stat method, data taken from previous work (*19*). (B) The columns show the pH−activity profile of *F. solani* pisi cutinase (0.06 μg/mL) measured with the ATR-FTIR method using a triolein film as a substrate. Experiments were performed in 3 × 50 mM citrate/tris-glycine (pH 3.5−10.5) buffer, at 25 °C in random order over 3 days with a relative standard deviation within 10%. The solid line is the protonation state of the His188 based on the experimentally determined pK_a of 5.0. The dashed line shows the theoretical protonation state based on the modeled pK_a of 6.6. (C) Columns show the pH−activity profile of *F. solani* pisi cutinase (0.74 μM) measured with NMR spectroscopy using propyl acetate as a substrate. Experiments were performed in 200 mM phosphate (pH 3.5−10.5) buffer, at 25 °C. The solid line shows the protonation state of the His188 based on the experimentally determined pK_a of 5.0. The dashed line shows the theoretical protonation state based on the modeled pK_a of 5.4.

RESULTS

Determination of the pH−Activity Profile of Cutinase. The pH−activity profile was obtained by measuring enzymatic activity of cutinase toward triolein in 0.5 pH steps over the pH range from 3.5 to 10.5 (Figure 1 B) on an ATR-FTIR spectrometer. During hydration without lipase, no or minor

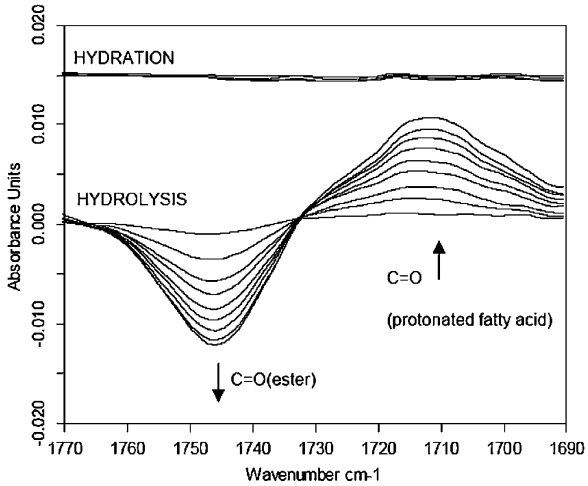

FIGURE 2: ATR-FTIR difference spectra during 5 min of hydration at pH 4 without lipase, $\Delta t = 1$ min (top set of spectra), and during 8 min of hydrolysis at pH 4 using cutinase, $\Delta t = 1$ min (bottom set of spectra). The peak around 1745 cm^{-1} is assigned to the carbonyl stretching vibration in triolein (ester), and the peak near 1710 cm^{-1} is assigned to the carbonyl stretching vibration in protonated oleic acid (carboxylic acid). The arrows illustrates the temporal progress of the peaks. Note that the hydration spectra were shifted (+0.015 absorbance unit) to improve comparison with the hydrolysis spectra.

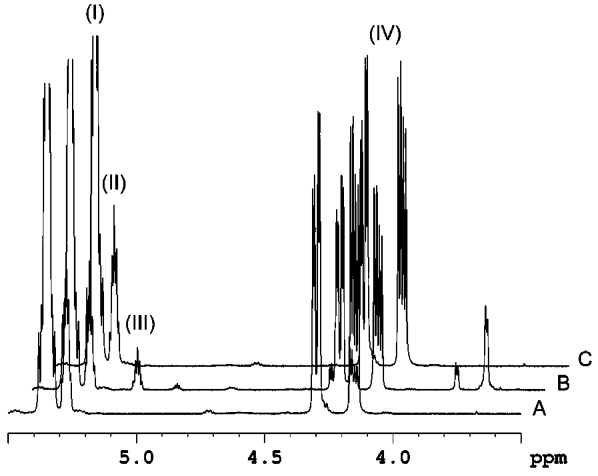

FIGURE 3: Segment of 1D proton NMR spectra, taken after (A) degradation for 0 h and (B) degradation for 120 min at pH 6. (C) Sample stored for >20 h in buffer (pH 6). The detected peaks come from (I) CH═CH hydrogen atoms of the oleic acid side chain, (II) the central hydrogen atom (H-2) of the glycerol backbone of triolein, and (III) the central hydrogen atom (H-2) of the glycerol backbone of 1,2-diolein. (IV) This region from 4.5 to 3.5 ppm contains peaks from the other glycerol backbone hydrogen atoms.

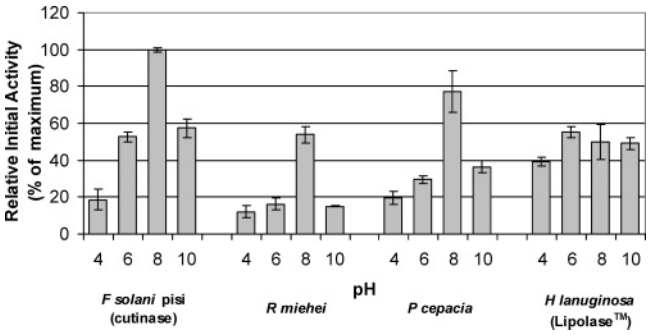

FIGURE 4: pH−activity profiles of four lipases from *F. solani* pisi (cutinase), *R. miehei*, *P. cepacia*, and *H. lanuginosa* (lipolase) using triolein as a substrate. Activity was measured utilizing the ATR-FTIR method with a triolein film as a substrate. The measurements were performed at 30 °C in a 3 × 50 mM citrate/tris-glycine buffer at pH 4, 6, 8, and 10. The concentration of the lipases was 5 μg/mL in all experiments.

spectral changes were observed, while after addition of lipase, the magnitude of the carbonyl ester band at 1745 cm^{-1} decreases and simultaneously the magnitude of the carbonyl vibration stemming from protonated oleic acid (1710 cm^{-1}) increases (Figure 2). The pH profile revealed the pH optimum for cutinase at pH 8.5 and significant amounts of enzymatic activity over the whole pH range that was examined (pH 3.5−10.5). Even at pH 3.5, cutinase exhibited more than 10% of the maximum activity (at the pH optimum of 8.5). In the neutral and alkaline pH range, the curve shape of the pH−activity profile of cutinase obtained by FTIR resembled closely the profile measured with the pH-stat method (Figure 1A,B). At pH values lower than 5, it is no longer possible to measure the activity in real time with the pH-stat method as the pH drops below the pK_a of the substrate.

To verify the acid activity of cutinase, the hydrolysis of triolein also was assessed at pH 4 and 6 using NMR spectroscopy (Figure 3). The result shows that cutinase still retains its hydrolytic capability at a pH as low as 4, with a hydrolysis rate of 3.2 ± 0.5 μmol min^{-1} mg^{-1} for pH 4 and a rate of 12.4 ± 0.7 μmol min^{-1} mg^{-1} for pH 6. Reference samples of triolein kept at pH 4 and 6 did not show any autohydrolysis that could be detected by the NMR, even after extended periods of time (>20 h).

The pH−activity profile for cutinase on a soluble ester, in this case propyl acetate, was measured using NMR spectroscopy (Figure 1C). The profile yields a pH optimum at pH 8 with a drop in activity when the pH is below 7. In a comparison with the data for triolein hydrolysis measured with ATR-FTIR, it is seen that the enzyme loses its ability to degrade the soluble substrate in the acidic range while its activity is retained with an insoluble substrate.

Determination of the pH−Activity Profile of Three Other Lipases in Comparison to Cutinase. The pH−activity profile of three commercial available lipases was measured on an ATR-FTIR spectrometer and compared to the profile from cutinase (Figure 4). *R. miehei* lipase and *P. cepacia* lipase display profile similar to that of cutinase even though the shapes of the curves are slightly different. All three of these lipases exhibit maximal activity in the alkaline pH range (~8). The fourth lipase (from *H. lanuginosa*), however, displayed its highest activity in the neutral pH range. Despite the slightly different pH optima, all the lipases used in this study exhibit significant enzymatic activity at pH 4. The activity at pH 4 taken as the amount of activity relative to the maximum activity for the individual activity is 18.6% for cutinase, 22.4% for *R. miehei* lipase, 25.3% for *P. cepacia* lipase, and 70.6% for *H. lanuginosa* lipase.

Determining the pK_a Value for the Active Site Histidine (His188) of Cutinase. To determine the pK_a of His188, the changes in chemical shift for the $C^{\epsilon 1}$−$H^{\epsilon 1}$ pair were followed from pH 3.3 to 8.4. The measured change in chemical shift for the $C^{\epsilon 1}$−$H^{\epsilon 1}$ pair shows a clear sigmoidal transition (Figure 5). The transition point is interpreted as the pK_a of the histidine, and it is determined to be 5.00 ± 0.02 by fitting the experimental data to a Henderson−Hasselbach equation.

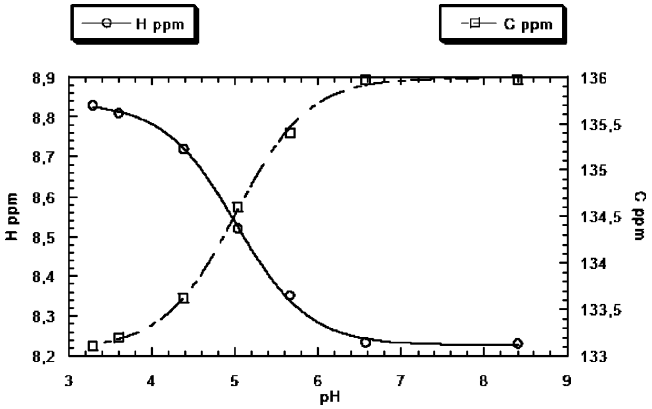

FIGURE 5: Transition curve for the titration of active site His188 of *F. solani* pisi cutinase. The chemical shifts of $C^{\epsilon 1}$ and $H^{\epsilon 1}$ are plotted as a function of the pH of the solution.

DISCUSSION

Lipolytic activity has been studied for decades. Although product formation can be readily detected either directly or indirectly, the atomic details of the enzymatic function have remained largely elusive. In contrast to enzymes working under isotropic conditions against a soluble substrate, the lipase is typically dependent on the presence of an interface between the lipidic substrate and the solvent water.

The FTIR method allows for detection of lipolytic activity under conditions that closely resemble natural conditions, where the lipid phase resembles a multilayer. We find unambiguous evidence for significant enzymatic activity all the way down to pH 3.5 (Figure 1B) for cutinase and to pH 4 for all the other lipases (Figure 4).

Comparing the pH−activity data from the degradation of soluble and insoluble esters (Figure 1B,C) shows an obvious difference in the acidic region (pH <5). Here the observed activity on a soluble ester is significantly lower than the activity determined for cutinase on an insoluble substrate, creating an oil−water interface. From this, it is also seen that the acid activity is only present when cutinase is working on a film substrate, indicating that the degradation route is not the same for the different substrates. This might very well be due to the difference in the way the substrate is presented to the enzyme.

To explain the observed acid activity on the lipid film substrate, information about the pK_a of the active site histidine (His188) side chain of cutinase is of interest. This has previously been estimated to be 5.9 (*30*), with a pK_a that is that high, we have been unable to explain the activity of cutinase at such a low pH as the catalytic mechanism is closely linked to the protonation state of the active site histidine. We determined the pK_a for His188 to be 5.0, and this correlates better with the experimentally detected acid activity of cutinase. However, in a comparison of the measured activity data with the protonation state of His188 (Figure 1B), it can be seen that the lower pK_a of His188 does not fully explain the acid activity, as the activity at very low pH is larger than expected. One parameter that could explain the acid activity would be a further shift of the His188 pK_a into the acidic range upon binding of substrate. Measuring this directly using NMR does not seem feasible, but a method of determining the pK_a of an active site histidine with the enzyme being active is to model the protonation/deprotonation curve on the measured activity data (*33*). This was done for cutinase activity on a lipid film, and the modeled transition curve yields a pK_a value for His188 of 6.6. A pK_a value in this range does little to explain the observed acid activity (Figure 1B). A similar comparison was carried out for the activity on the soluble substrate, yielding a pK_a of 5.4 for His188 (Figure 1C). Comparing the data for the soluble substrate with the experimentally determined pK_a of the His188 shows a good correlation, but in a comparison with the data from the lipid film, the modeled pK_a seems unrealistically high; we must therefore question the validity of values determined using this method on data from activity on insoluble substrates such as lipid films.

The polarity of the bulk solution has been shown to have an influence on the pK_a (*34*). In this case, the polarity will seem lower at the lipid interface, resulting in a preference of His over His^+ and can consequently account for some of the observed acid activity. This is also supported by the fact that the modeled pK_a from the soluble substrate does not deviate significantly from one measured using NMR spectroscopy, indicating that the polarity of the interface or the interface itself is responsible for the acid activity.

The current data are insufficient to fully explain the observed activity at acidic pH using the commonly accepted model for lipolytic activity where the protonation state of the active site histidine plays a crucial role. We therefore propose a model allowing the active site histidine to be deprotonated at acidic pH when acting on an interface.

pH in the Active Site. Normally, one considers enzyme systems macroscopically; i.e., one measures statistical properties of large ensembles, to obtain mean properties for physical observables. Statistically, a titratable residue may therefore carry a partial charge. In contrast, on the microscopic single-residue level, a residue is either charged or uncharged; no partial charges can exist. This distinction is important for understanding the protonation state of the active site of an enzyme. When substrate is present, the active site cleft of lipases will be closed by the lipidic layer and consequently there is no solvent access to the cavity. Similarly, Noinville et al. (*5*) has shown that lipase from *H. lanuginosa* upon binding to a surface of octadecyltrichlorosilane shows a remarkable increase in the protection of labile backbone NH pairs from exchange with D_2O in solution. As this is closely linked with the amount of lipase, they conclude that this effect is due to the packing of the protein molecules, but also and more interestingly, they conclude that H_2O molecules in or around the active site might be trapped by the binding of the lipase to the surface.

When the pH in the lipase active site is assessed, the average distance between two H_3O^+ molecules at pH 4 in bulk solution is approximately 250 Å, corresponding to a volume of 16.6×10^6 Å^3 per H_3O^+ molecule. A typical active site may exhibit dimensions on the order of 10 Å × 5 Å × 5 Å (250 Å^3). It is therefore unlikely to encounter two positively charged molecules in the active site simultaneously. If we consider probabilities, then the average amount of hydroxonium ions populating the active site with a volume

of 250 Å^3 is at pH 4

$$p = 250\ \text{Å}^3/(16.6 \times 10^6\ \text{Å}^3\ \text{per}\ H_3O^+\ \text{molecule}) = 15.1 \times 10^{-6}\ H_3O^+\ \text{molecules}$$

In the solvent assessable state, the active site His is protonated at acidic pH values and its positive charge will prevent the entry of an H_3O^+ molecule into the active site due to electrostatic repulsion. In the solvent inaccessible state of the active site, it is likely it displays a His^+ and not concurrently a H_3O^+ or a His and H_3O^+.

The active site His will now establish a local equilibrium

$$H_2O + His^+ \rightleftarrows H_3O^+ + His$$

and in its deprotonated form, it is capable of facilitating catalysis. When the active site is freely accessible to solvent, chemical communication with ionized species, such as the hydronium ion in the bulk solution, will result in the active site residues regaining the protonation state dictated by bulk pH. In contrast, when chemical communication between the bulk solvent and the active site is prevented by lipid closure or by aggregated substrate, we postulate that only one positively charged entity can reside in the active site at any point in time. Thus, the conventional definition of pH is not applicable, because of the lack of chemical communication with bulk solvent.

These considerations represent a de facto quantization of pH in the active site of enzymes where the active site volume is inaccessible to the solvent.

Very Small Restricted Volumes and pH. The effect of this is not limited to the interaction of cutinase with a lipid film substrate, but will be true for all significantly small volumes alternating between an open and closed form. In such a case, the inclusion or exclusion of one H_3O^+ in the restricted volume will have a significant influence on the resulting pH. The effect of this compartmentalization is that the pH in the small restricted volume can only assume discrete values; the pH has in effect become quantized. As this will have a significant influence on the perceived pH of the restricted volume, the size of the restricted volume where this comes into play becomes interesting.

A measure of this is the change in pH in the restricted volume ($\Delta pH_{n,V_r}$) as a function of the number of H_3O^+ molecules trapped in the restricted volume in addition to the bulk pH contribution (n) and the size of the restricted volume (V_r). We defined $\Delta pH_{n,V_r}$ as

$$\Delta pH_{n,V_r} = pH_{bulk} - pH_{n,V_r}$$

where $\Delta pH_{n,V_r}$ is given by the difference in pH from the bulk pH (pH_{bulk}) to the pH in the restricted volume (pH_{n,V_r}). pH_{n,V_r} is in turn defined as the pH of the restricted volume based on the bulk pH contribution and the additional (n) H_3O^+ trapped in it.

$$pH_{n,V_r} = -\log\left([H_{bulk}{}^+] + \frac{n}{N_A V_r}\right)$$

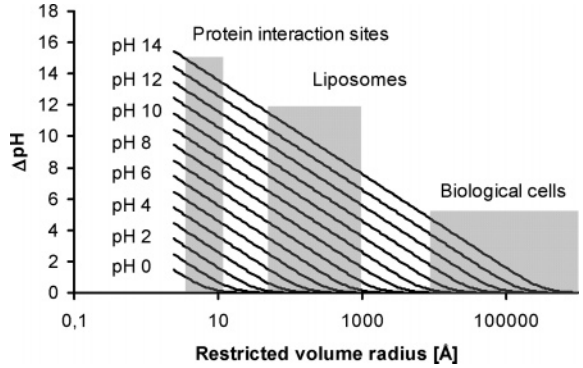

FIGURE 6: Theoretical change in the pH of the restricted volume compared to bulk pH by inclusion of one additional H_3O^+ plotted as a function of the radius of the restricted volume.

where N_A is Avogadro's number. This can then be combined and rewritten

$$\Delta pH_{n,V_r} = pH_{bulk} + \log\left(\frac{n}{N_A V_r} + 10^{-pH_{bulk}}\right)$$

When the case in which $n = 1$ is examined (Figure 6), it is seen that for neutral pH the change in pH is indeed significant for a wide range of restricted volume sizes. It must be noted that this does in no way take into account any buffer effects present in the system, nor does it take into account the probability of such an event.

The wide implications of this proposal are very interesting. Aside from very small active site volumes, biology is rich in compartments of almost arbitrary sizes. Nanosomes and liposomes represent just two such cases. As can be seen from Figure 6, dramatic ΔpH values can be obtained in such compartments at biologically relevant pH values, simply due to restricted chemical communication.

Chemical Communication (with) in the Solvent. In a simplified view, this implies that the active site alternates between a filled, nonaccessible state and an empty, accessible state. Thus, the open, accessible state of cutinase has ample time of equilibration with bulk solvent, while being open (devoid of substrate). In the closed form (substrate populated), the active site is only influenced indirectly by the titration state of titratable residues on the protein surface.

pH is a macroscopic statistical property which does not pertain to the active site environment of an individual enzyme molecule. Our claim is thus that the enzyme is perfectly capable of communicating chemically with the hydronium ions while in an isotropic solution. Conversely, under conditions where water access to the active site is hindered by, for example, binding to the lipidic interface, chemical communication is effectively blocked. Indirect effects from protonation/deprotonation of titratable surface residues may still influence, for example, the effective pK_a values of the active site residues, since the surrounding electrostatic field will penetrate the molecule independent of its binding to the lipidic interface.

This work presents important new observations on lipolytic activity under acidic conditions. It also proposes a new view of pH in the active site environment, where the lack of chemical communication, due to compartmentalization, will make changes in hydronium ion concentration a discrete event. There is only a certain probability of finding one

hydronium ion; it is exceedingly improbable to find two simultaneously.

ACKNOWLEDGMENT

We thank Sebastian Schellbach for his involvement in parts of the NMR work and Dr. Kim Borch, Dr. Claus C. Fuglsang, and Dr. S. A. Patkar (Novozymes) for the supply of highly purified *H. lanuginosa* lipase.

REFERENCES

1. Kirk, O., Borchert, T. V., and Fuglsang, C. C. (2002) Industrial enzyme applications, *Curr. Opin. Biotechnol. 13*, 345−51.
2. Ollis, D. L., Cheah, E., Cygler, M., Dijkstra, B., Frolow, F., Franken, S. M., Harel, M., Remington, S. J., Silman, I., and Schrag, J. (1992) The α/β hydrolase fold, *Protein Eng. 5*, 197−211.
3. Brzozowski, A. M., Derewenda, U., Derewenda, Z. S., Dodson, G. G., Lawson, D. M., Turkenburg, J. P., Bjorkling, F., Huge-Jensen, B., Patkar, S. A., and Thim, L. (1991) A model for interfacial activation in lipases from the structure of a fungal lipase-inhibitor complex, *Nature 351*, 491−4.
4. Jutila, A., Zhu, K., Patkar, S. A., Vind, J., Svendsen, A., and Kinnunen, P. K. (2000) Detergent-induced conformational changes of *Humicola lanuginosa* lipase studied by fluorescence spectroscopy, *Biophys. J. 78*, 1634−42.
5. Noinville, S., Revault, M., Baron, M. H., Tiss, A., Yapoudjian, S., Ivanova, M., and Verger, R. (2002) Conformational changes and orientation of *Humicola lanuginosa* lipase on a solid hydrophobic surface: An in situ interface Fourier transform infrared-attenuated total reflection study, *Biophys. J. 82*, 2709−19.
6. Jorgensen, S., Skov, K. W., and Diderichsen, B. (1991) Cloning, sequence, and expression of a lipase gene from *Pseudomonas cepacia*: Lipase production in heterologous hosts requires two *Pseudomonas* genes, *J. Bacteriol. 173*, 559−67.
7. Boel, E., Huge-Jensen, B., Christensen, M., Thim, L., and Fiil, N. P. (1988) *Rhizomucor miehei* triglyceride lipase is synthesized as a precursor, *Lipids 23*, 701−6.
8. Derewenda, U., Swenson, L., Wei, Y., Green, R., Kobos, P. M., Joerger, R., Haas, M. J., and Derewenda, Z. S. (1994) Conformational lability of lipases observed in the absence of an oil−water interface: Crystallographic studies of enzymes from the fungi *Humicola lanuginosa* and *Rhizopus delemar*, *J. Lipid Res. 35*, 524−34.
9. Martinez, C., Nicolas, A., van Tilbeurgh, H., Egloff, M. P., Cudrey, C., Verger, R., and Cambillau, C. (1994) Cutinase, a lipolytic enzyme with a preformed oxyanion hole, *Biochemistry 33*, 83−9.
10. Longhi, S., Czjzek, M., Lamzin, V., Nicolas, A., and Cambillau, C. (1997) Atomic resolution (1.0 Å) crystal structure of *Fusarium solani* cutinase: Stereochemical analysis, *J. Mol. Biol. 268*, 779−99.
11. Chahinian, H., Nini, L., Boitard, E., Dubes, J. P., Comeau, L. C., and Sarda, L. (2002) Distinction between esterases and lipases: A kinetic study with vinyl esters and TAG, *Lipids 37*, 653−62.
12. Schrag, J. D., Li, Y., Cygler, M., Lang, D., Burgdorf, T., Hecht, H. J., Schmid, R., Schomburg, D., Rydel, T. J., Oliver, J. D., Strickland, L. C., Dunaway, C. M., Larson, S. B., Day, J., and McPherson, A. (1997) The open conformation of a *Pseudomonas* lipase, *Structure 5*, 187−202.
13. Derewenda, Z. S., Derewenda, U., and Dodson, G. G. (1992) The crystal and molecular structure of the *Rhizomucor miehei* triacylglyceride lipase at 1.9 Å resolution, *J. Mol. Biol. 227*, 818−39.
14. Brzozowski, A. M., Savage, H., Verma, C. S., Turkenburg, J. P., Lawson, D. M., Svendsen, A., and Patkar, S. (2000) Structural origins of the interfacial activation in *Thermomyces* (*Humicola*) *lanuginosa* lipase, *Biochemistry 39*, 15071−82.
15. Carvalho, C. M., Aires-Barros, M. R., and Cabral, J. M. (1999) Cutinase: From molecular level to bioprocess development, *Biotechnol. Bioeng. 66*, 17−34.
16. Tiss, A., Carriere, F., and Verger, R. (2001) Effects of gum arabic on lipase interfacial binding and activity, *Anal. Biochem. 294*, 36−43.
17. Crooks, G. E., Rees, G. D., Robinson, B. H., Svensson, M., and Stephenson, G. R. (1995) Comparison of hydrolysis and esterification behavior of *Humicola langinosa* and *Rhizomucor miehei* lipases in AOT-stabilized water-in-oil microemulsions. 1. Effect of pH and water content on reaction kinetics, *Biotechnol. Bioeng. 48*, 78−88.
18. Svendsen, A., Borch, K., Barfoed, M., Nielsen, T. B., Gormsen, E., and Patkar, S. A. (1995) Biochemical properties of cloned lipases from the *Pseudomonas* family, *Biochim. Biophys. Acta 1259*, 9−17.
19. Neves-Petersen, M. T., Petersen, E. I., Fojan, P., Noronha, M., Madsen, R. G., and Petersen, S. B. (2001) Engineering the pH-optimum of a triglyceride lipase: From predictions based on electrostatic computations to experimental results, *J. Biotechnol. 87*, 225−54.
20. Desnuelle, P. (1961) Pancreatic lipase, *Adv. Enzyme Regul. 23*, 129−61.
21. Kanicky, J., Poniatowski, A., Mehta, N., and Shah, D. (2000) Cooperativity among molecules at interfaces in relation to various technological processes: Effect of chain length on the pK_a of fatty acid salt solutions, *Langmuir 16*, 172−7.
22. Christodoulou, A. P., and Rosano, H. L. (1968) Effects of pH and Nature of Monovalant Cations on Surface Isotherms of Saturated C16 to C22 Soap Monolayers, *Adv. Chem. Ser. 84*, 210−34.
23. Kanicky, J. R., and Shah, D. O. (2002) Effect of degree, type, and position of unsaturation on the pK_a of long-chain fatty acids, *J. Colloid Interface Sci. 256*, 201−7.
24. Snabe, T., Neves Petersen, M. T., and Petersen, S. B. (2005) Enzymatic Lipid Desorption by a pH-induced "Electrostatic Explosion", *Chem. Phys. Lipids 133*, 37−49.
25. Winkler, U. K., and Stuckmann, M. (1979) Glycogen, hyaluronate, and some other polysaccharides greatly enhance the formation of exolipase by *Serratia marcescens*, *J. Bacteriol. 138*, 663−70.
26. Gupta, R., Rathi, P., Gupta, N., and Bradoo, S. (2003) Lipase assays for conventional and molecular screening: An overview, *Biotechnol. Appl. Biochem. 37*, 63−71.
27. Snabe, T., and Petersen, S. B. (2002) Application of infrared spectroscopy (attenuated total reflection) for monitoring enzymatic activity on substrate films, *J. Biotechnol. 95*, 145−55.
28. Edgcomb, S. P., and Murphy, K. P. (2002) Variability in the pK_a of histidine side-chains correlates with burial within proteins, *Proteins 49*, 1−6.
29. Plesniak, L. A., Connelly, G. P., Wakarchuk, W. W., and McIntosh, L. P. (1996) Characterization of a buried neutral histidine residue in *Bacillus circulans* xylanase: NMR assignments, pH titration, and hydrogen exchange, *Protein Sci. 5*, 2319−28.
30. Prompers, J. J., Groenewegen, A., Hilbers, C. W., and Pepermans, H. A. (1999) Backbone dynamics of *Fusarium solani* pisi cutinase probed by nuclear magnetic resonance: The lack of interfacial activation revisited, *Biochemistry 38*, 5315−27.
31. Mori, S., Abeygunawardana, C., Johnson, M. O., and van Zijl, P. C. (1995) Improved sensitivity of HSQC spectra of exchanging protons at short interscan delays using a new fast HSQC (FHSQC) detection scheme that avoids water saturation, *J. Magn. Reson., Ser. B 108*, 94−8.
32. Prompers, J. J., Groenewegen, A., Van Schaik, R. C., Pepermans, H. A., and Hilbers, C. W. (1997) ^{1}H, ^{13}C, and ^{15}N resonance assignments of *Fusarium solani* pisi cutinase and preliminary features of the structure in solution, *Protein Sci. 6*, 2375−84.
33. Masson, P., Nachon, F., Bartels, C. F., Froment, M. T., Ribes, F., Matthews, C., and Lockridge, O. (2003) High activity of human butyrylcholinesterase at low pH in the presence of excess butyrylthiocholine, *Eur. J. Biochem. 270*, 315−24.
34. Fersht, A. (1999) *Structure and mechanism in protein science*, 3rd ed., W. H. Freeman, New York.

BI050634O